2020

Deep Learning Models In Detecting Pathologies In Chest-Xray

DURGA PRASAD, AKAASH, SURESH, NITISH, KARTHIK

1.Introduction:

Across the globe respiratory-related diseases claim most of the lives and there is a wide variety of pathologies that cause respiratory diseases. The Deep learning models trained on natural images are commonly used for different classification tasks in the medical domain. We develop a model that can detect various pathogens from chest X-rays at a level in par with practicing radiologists. In the current model, we are aiming to train the model using deep learning approaches. Convolutional Neural Network (CNN) has gained popularity in learning mid and high-level representations. We explore this capability of CNN deep learning architectures to identify various pathologies in the chest x-ray images. The final trained model will take an Xray input and will be able to classify and predict the presence of a particular pathogen. The model will also be used to classify the latest virus which is causing chaos over the world the novel coronavirus COVID-19 which affected more than 4.44m people and claiming 302k+ lives as of 15th May 2020.

Following are the class of pathologies the model can classify by taking the input chest x-ray image

1.	Atelectasis	9.	Consolidation
2.	Cardiomegaly	10.	Edema
3.	Effusion	11.	Emphysema
4.	Infiltration	12.	Fibrosis
5.	Mass	13.	Pleural_Thickening
6.	Nodule	14.	Hernia
7.	Pneumonia	15.	Coronavirus COVID-19
8.	Pneumothorax		

Chest radiographs are the very common diagnostic imaging tool used across the hospitals in identifying the chest abnormalities. Brief description of each Pathology is provided below with sample representation chest radiograph.

Chest Xray Interpretation

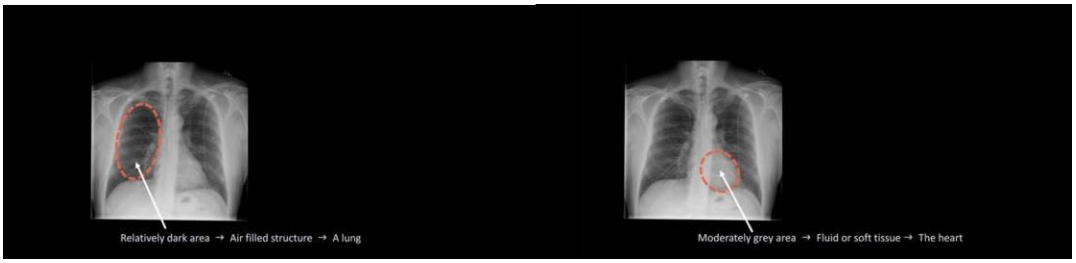

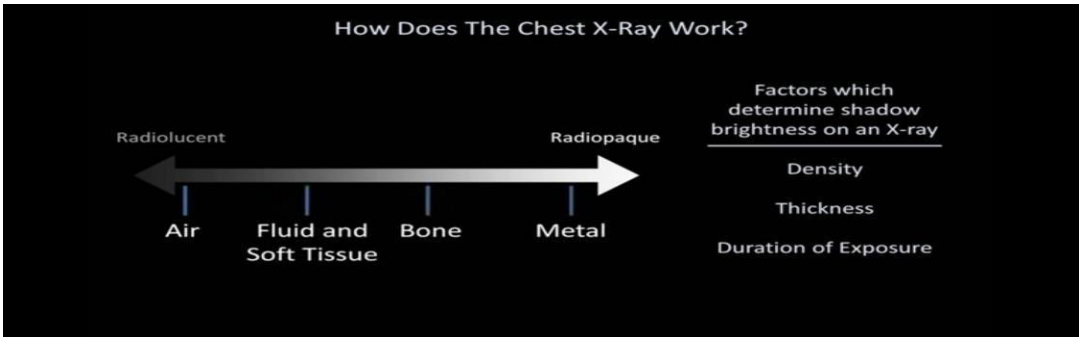

Chest Xray views

- PA View
  The x-ray source is positioned so that the x-ray beam enters through the posterior (back) aspect of the chest and exits out of the anterior (front) aspect, where the beam is detected.

- AP View
  the positions of the x-ray source and detector are reversed: the x-ray beam enters through the anterior aspect and exits through the posterior aspect of the chest.

- Lateral View
  Here the patient stands with both arms raised and the left side of the chest pressed against a flat surface.

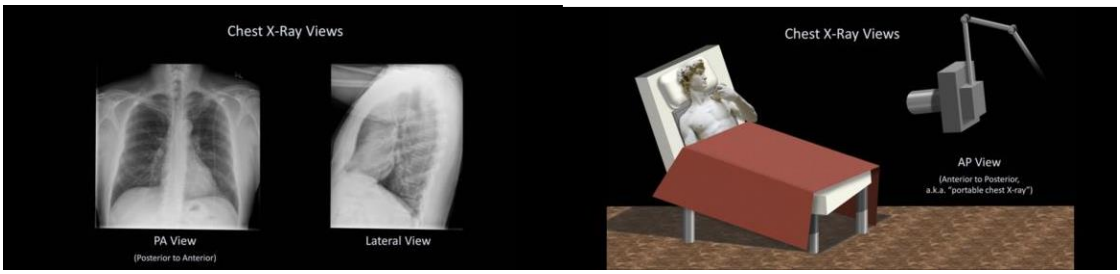

1.1 Atelectasis:

Atelectasis (refer Fig 1.1) is another word for lung collapse [1]. The commonest cause is a bronchial obstruction that results in distal gas resorption and a reduction in the volume of gas in the affected lung, lobe, segment or subsegment. As the gas is resorbed, the walls of the alveoli collapse in on themselves and the size of the affected area reduces.

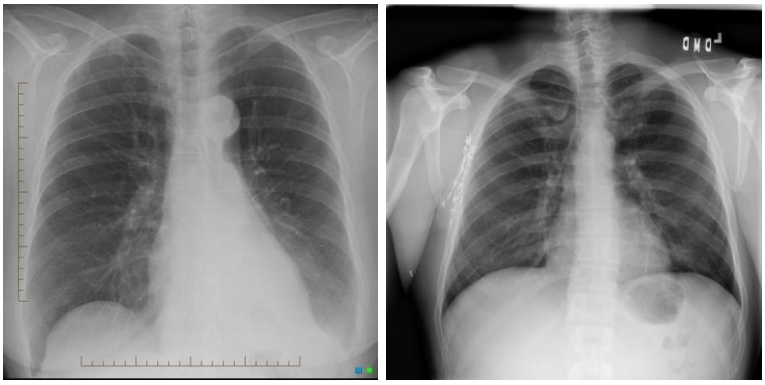

Fig. 1.1. Atelectasis

1.2. Cardiomegaly:

Cardiomegaly means enlargement of the heart [2]. The definition is when the transverse diameter of the cardiac silhouette is greater than or equal to 50% of the transverse diameter of the chest (increased cardiothoracic ratio) on a posterior-anterior projection of a chest radiograph or a computed tomography.

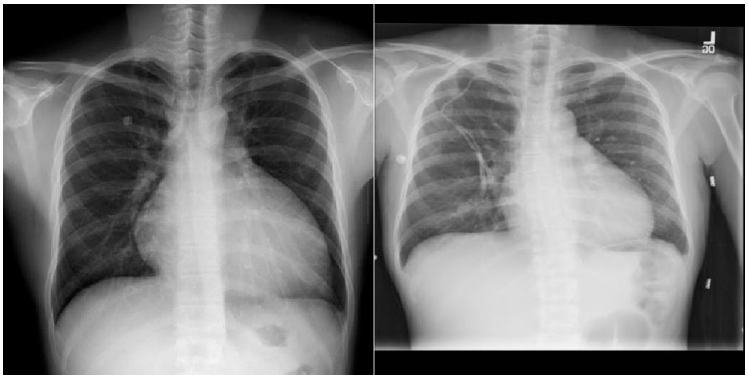

Fig 1.2. Cardiomegaly

1.3 Effusion

A pleural effusion is an abnormal collection of fluid in the pleural space resulting from excess fluid production or decreased absorption or both [3].

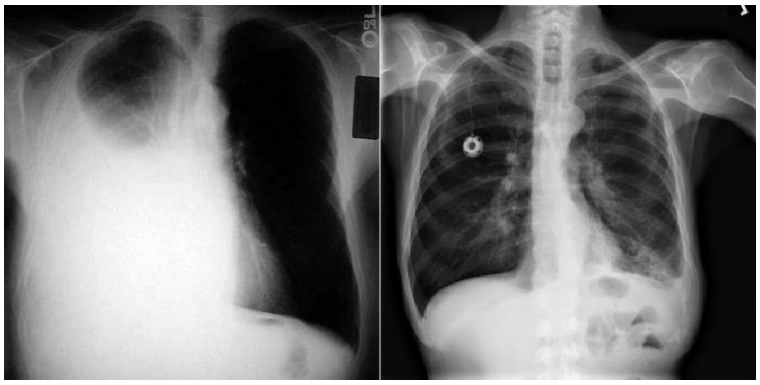

Fig.1.3. Effusion

1.4 Infiltration

Persistent pulmonary infiltrate results when a substance denser than air (e.g., pus, oedema, blood, surfactant, protein, or cells) lingers within the lung parenchyma. Non-resolving and slowly resolving pneumonias are the most common broad categories of persistent pulmonary infiltrate.

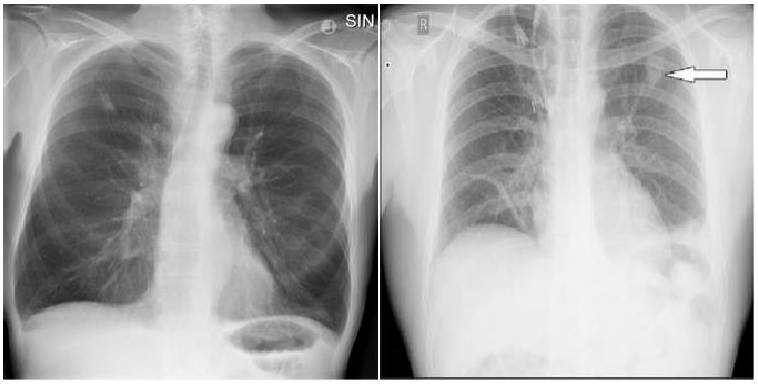

Fig 1.4.a Chest X-ray showing infiltrate in the right lung.

Fig 1.4.b Chest X-ray image. Local infiltration in the upper lobe of the left lung (white arrow)

1.5 Mass:

Lung cancer is a mass or growth in the lung made up of cancer cells, but not all masses in the lung are caused by cancer. Lung masses and growths generally fall under two categories:

- Benign growths (non-cancerous)
- Malignant growths (cancerous)

Malignant masses are often larger than benign nodules. Malignant masses are also more likely to show up in certain parts of your lung.

Fig. 1.5 Lung Mass

1.6 Nodule:

Usually, the first sign that a pulmonary nodule is present is a spot on the lung that shows up on a chest X-ray or a CT scan.

Single pulmonary nodules seen on chest x-rays are generally at least 8 to 10 millimeters in diameter. If they are smaller than that, they are unlikely to be visible on a chest X-ray. The larger the nodule is, and the more irregularly shaped it is, the more likely it is to be cancerous. Those located in the upper portions of the lung are also more likely to be cancerous.

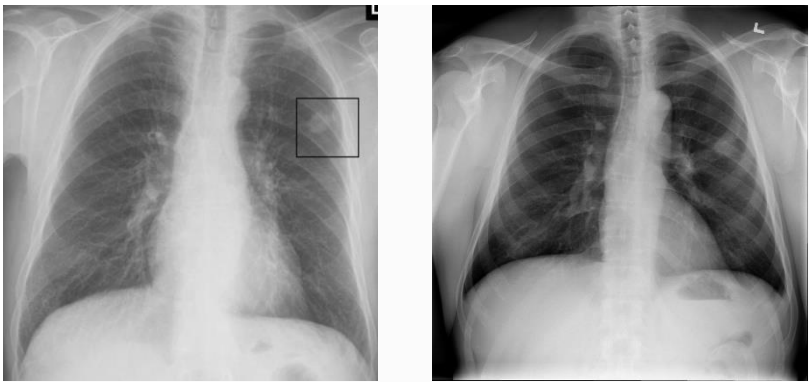

Fig. 1.6 Lung Nodule

1.7 Pneumonia

Infection that inflames air sacs in one or both lungs, which may fill with fluid. With pneumonia, the air sacs may fill with fluid or pus. The infection can be life-threatening to anyone, but particularly to infants, children, and people over 65.

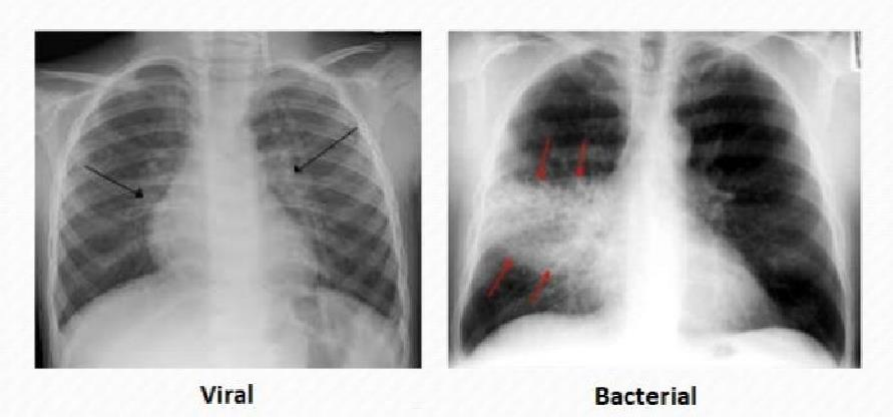

Fig. 1.7 Pneumonia

1.8 Pneumothorax /collapsed lung

It is a condition that occurs when air enters the space between the chest wall and the lung (Pleural space) and causes a collapsed lung. Pneumothorax can be a complete lung collapse or a collapse of only a portion of the lung.

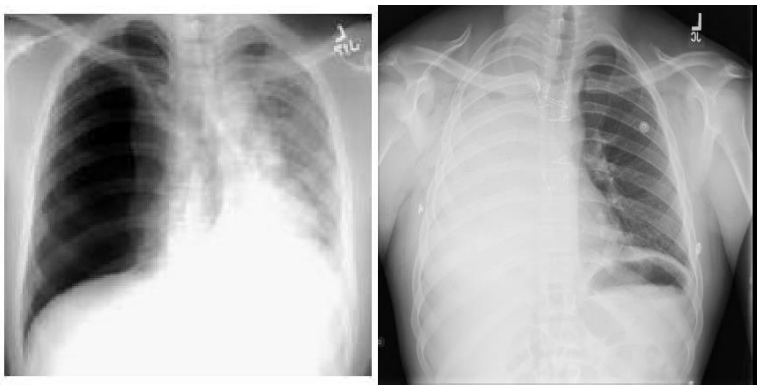

Fig. 1.8. Pneumothorax (left lung is collapsed)

1.9 Consolidation

A pulmonary consolidation is a region of normally compressible lung tissue that has filled with liquid instead of air. Consolidation occurs through the accumulation of inflammatory cellular exudate in the alveoli and adjoining ducts. The liquid can be pulmonary edema, inflammatory exudate, pus, inhaled water, or blood (from bronchial tree or hemorrhage from a pulmonary artery).

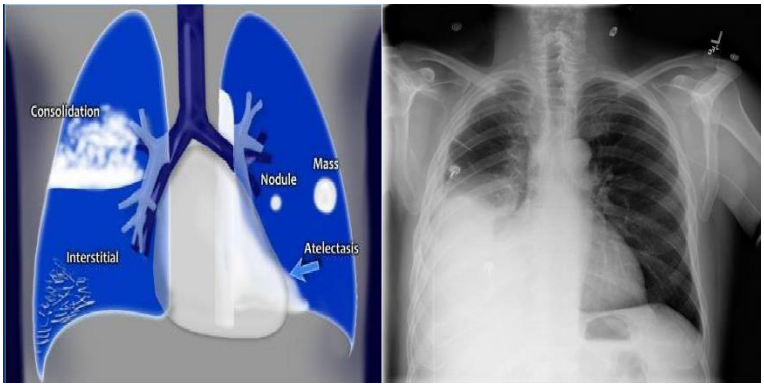

Fig. 1.9. Consolidation (right lung)

1.10 Edema

Pulmonary edema is a condition that is caused by accumulation of excess fluid in the lungs [10]. This condition results in breathing difficulties as the fluid gets accumulated in the lungs air sacs. This Fluid accumulation is caused due to multiple reasons like congestive heart failure, pneumonia, exposure to certain toxins, trauma to the chest wall etc. (Refer to Figure 1.10)

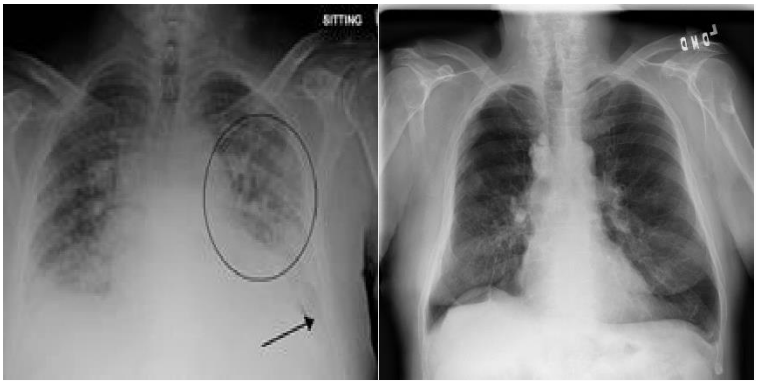

Fig. 1.10 Edema

1.11 Emphysema

Pulmonary Emphysema is a condition in which the air sacs of the lungs are damaged and enlarged, causing breathlessness [9]. Emphysema belongs to a group of lung diseases known as chronic obstructive pulmonary disease. Once it develops, emphysema cannot be reversed. When emphysema develops, the alveoli and lung tissue are destroyed & oxygen movement into the bloodstream will be reduced.

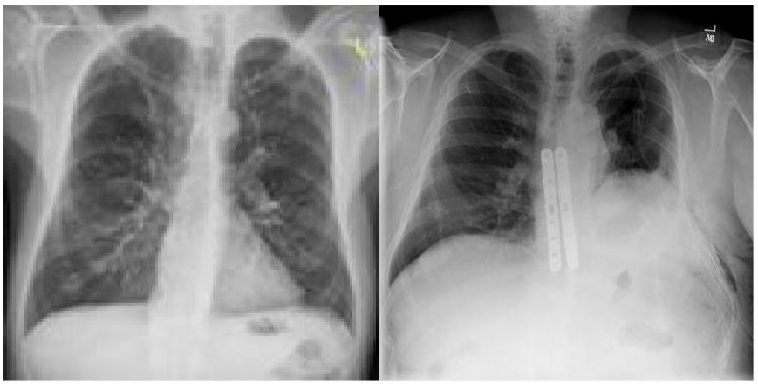

Fig 1.11 Emphysema

1.12 Fibrosis

Pulmonary fibrosis is a condition that occurs when the lung tissue becomes damaged and scarred [11]. Pulmonary fibrosis scars and thickens the tissue around and between the air sacs. This lung damage makes it difficult for the lungs to function properly. The damage caused to the lungs cannot be repaired and as the condition worsens, lungs become shorter of breath (Refer to Figure 1.12).

Fig. 1.12 Fibrosis

1.13 Pleural_Thickening:

Pleural thickening is a common finding on routine chest X-rays. It typically involves the apex of the lung, which is called 'pulmonary apical cap'. On chest X-rays, the apical cap is an irregular density located at the extreme apex and is less than 5 mm in width. Four areas of the lung (apical, upper, middle, and lower portions) were examined bilaterally for the presence of pleural thickening.

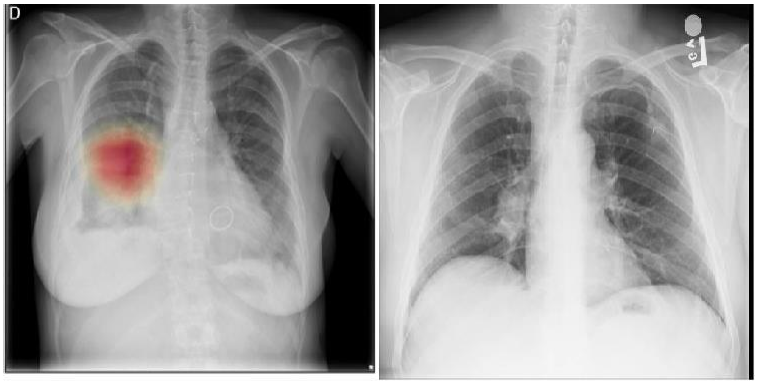

Fig 1.13 Pleural Thickening

1.14 Hernia:

A hernia occurs when an organ pushes through an opening in the muscle or tissue that holds it in place.

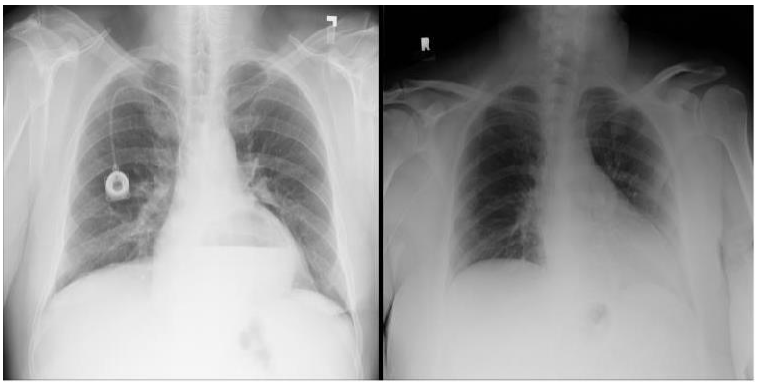

Fig 1.14. Hernia

1.15 Covid-19:

COVID-19 is a viral disease also known as SARS-CoV-2 or severe acute respiratory syndrome coronavirus 2. In humans, several coronaviruses are known to cause respiratory infections ranging from the common cold to more severe diseases such as Middle East Respiratory Syndrome (MERS) and Severe Acute Respiratory Syndrome (SARS). The most recently discovered coronavirus causes coronavirus disease COVID-19.

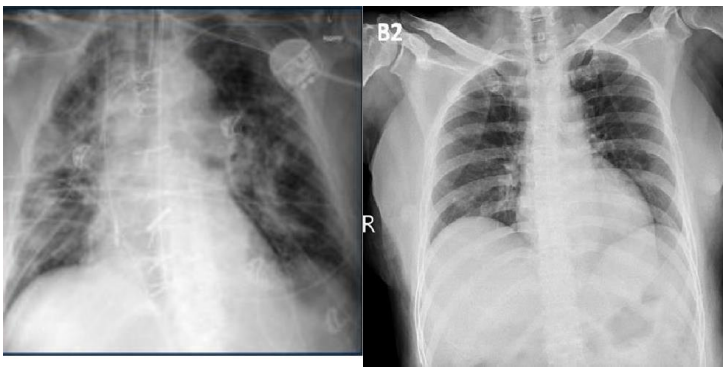

Fig.1.15.1 COVID-19

Covid-19 vs Pneumonia:

Fig.1.15.3 shows the difference between a few COVID and pneumonia case images. The following primary findings are frequently observed in the chest X-rays of COVID-19 patients.

- Ground-glass opacities (GGO) (bilateral, multifocal, subpleural, peripheral, posterior, medial and basal).
- A crazy paving appearance (GGOs and inter-/intra-lobular septal thickening).
- Air space consolidation.
- Bronchovascular thickening (in the lesion).
- Traction bronchiectasis.

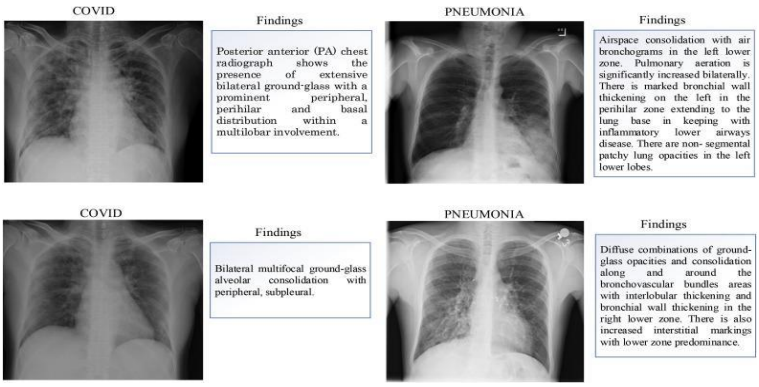

Fig.1.15.2 Differences observed by the radiologist between some COVID and pneumonia case images.

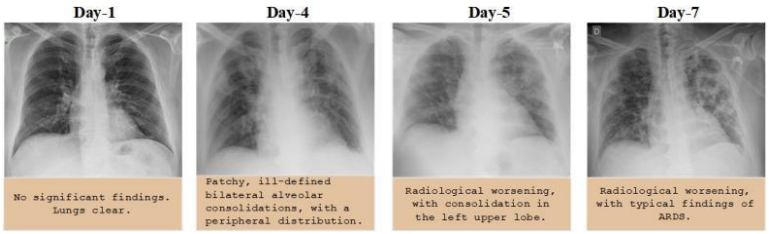

Fig.1.15.3 Chest X-ray images of a 50-year-old COVID-19 patient with pneumonia over a week

1.16 Normal:

Our model will be trained with chest X-ray images which are classified as normal.

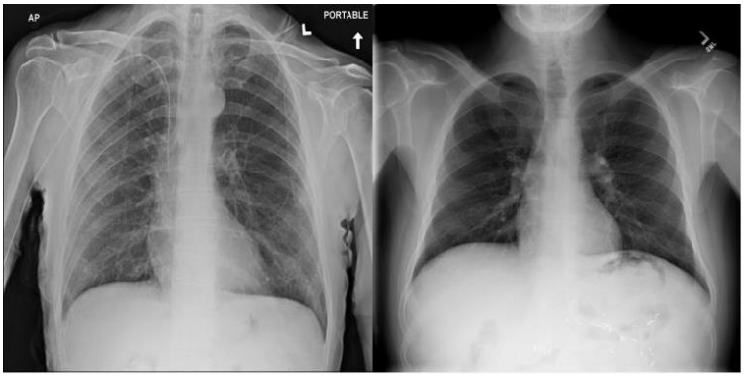

Fig.1.16 Normal chest Xray

2.Literature Survey:

More than 1 million adults are hospitalized with pneumonia and around 50,000 die from the disease every year in the US alone. Chest X-rays are currently the best available method for diagnosing pneumonia, playing a crucial role in clinical care [13] and epidemiological studies [12]. However, detecting pneumonia in chest X-rays is a challenging task that relies on the availability of expert radiologists.

X-rays produced worldwide are analyzed visually on scan by scan basis. It requires relatively high degree of accuracy. It is time-consuming, expensive and is prone to manual bias or wrong interpretation. Errors and delay in these diagnostic methods still contribute to a large number of patient deaths in hospitals, making these errors one of the largest causes of death along with heart disease and cancer.

2.1 Deep Learning:

Deep Learning is an extension to classical Machine Learning by adding depth to the model and also it transforms the data using various functions that allows data representation in a hierarchal way. Because of this complex model DL can solve the complex problems in a faster way with increased classification accuracy or a reduced regression errors, provided the large data sets are available for the given problem.

Convolutional Neural Networks (CNN) constitute a class of deep, feed-forward ANN performs different convolutions at different layers of the network and creates different representations of the learning data set. The convolutional layers act as feature extractors and then the pooling layer reduce the dimensions.

The main advantage of the DL especially while processing the images are the reduced need for the feature Engineering. Prior to the DL the traditional methods for image classification had to do a lot of hand engineered feature engineering and also based on the problem the feature engineering should be varied and it is proved to be a time consuming and expensive approach and also heavily dependent on the expert's domain knowledge. Densenet improves the flow of information and gradients throughout the network.

A disadvantage of DL is, it is data hungry model and requires huge data sets to learn and also sometimes require longer training times.

2.2 Available architectures and tools:
There exists pretrained architectures, which can be used to start building the models instead of starting the model creation from scratch. These pretrained models include AlexNet, Caffenet, VGG, GoogleNet, Inception, ResNet. All of these models come with their weights pre-trained, which basically means they are already trained using some data sets and has already learnt.

Apart from this pretrained models there are existing platforms which allows us to experiment with DL. The most popular ones are Theano, Tensorflow, Keras, Pytorch etc.

CheXNet model [6] used 121-layer Dense Convolutional Network (DenseNet) [14] trained on the ChestX-ray 14 dataset. DenseNets improve flow of information and gradients through the network, making the optimization of very deep networks tractable. They replaced the final fully connected layer with one that has a single output, after which they applied a sigmoid nonlinearity.

The weights of the CheXNet model network were initialized with weights from a model pretrained on ImageNet (Deng et al.,2009). The network was trained end-to-end using Adam with standard parameters (beta1 = 0:9 and beta2 = 0:999) [16]. They trained the model using mini batches of size 16. They used an initial learning rate of 0:001 that was decayed by a factor of 10 each time the validation loss plateaus after an epoch, and picked the model with the lowest validation loss.

3.The Model Architecture

The proposed model (Refers to figure 3.1& 3.2.) will contain multiple convolutional and pooling layers for feature extraction and then a flatten layer that connects to a fully connected layer. Figure 2.1 is only for the depiction purpose of the proposed model and the actual model, number of convolutions, pooling layers, fully connected layers will differ based on the further work and tuning of the model. We are also aiming at experimenting with the transferred learning and use pre-trained models (refer to figure 3.3).

For our study we are going to depend on Keras with Tensorflow. Tensorflow is much adapted model in production and scalability purposes. For evaluating the performance of our model, we will use precision and recall scoring metrics.

3.1Tentative list of Algorithms

VGG16, ResNet50, InceptionV3, Xception

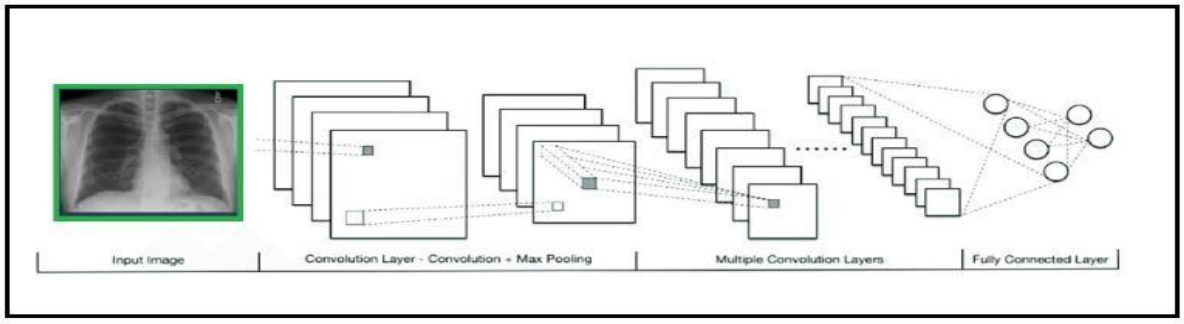

Fig. 3.1 Overview of Convolutional Neural Network (CNN) Architecture for pathology detection

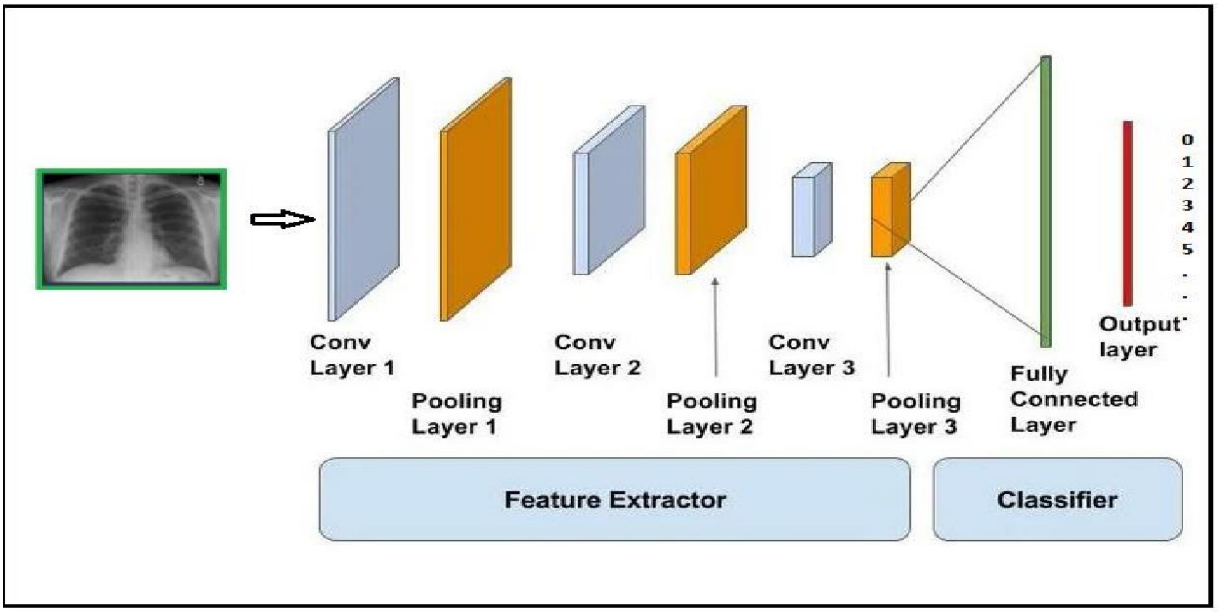

Fig. 3.2 Overview of Convolutional Neural Network (CNN) Architecture for pathology detection

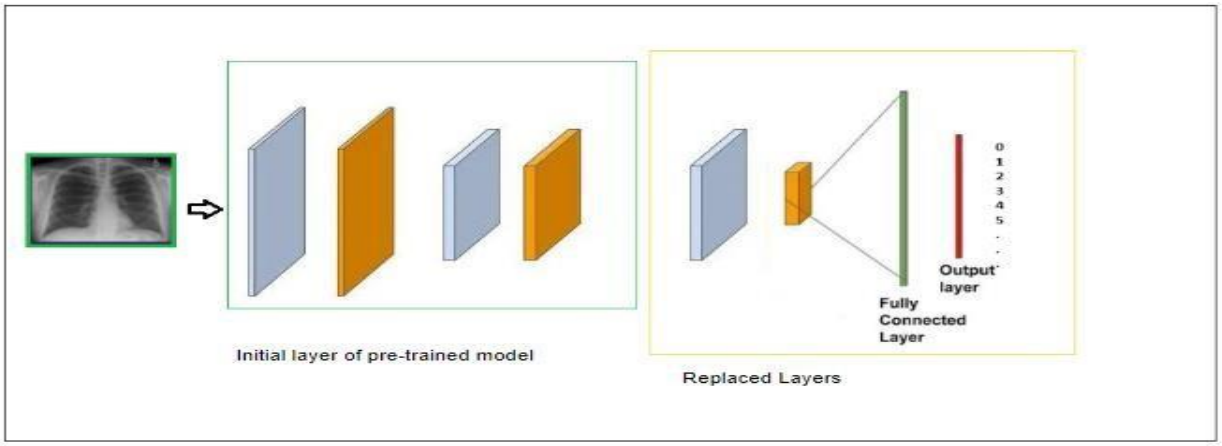

Fig. 3.3 Convolutional Neural Network (CNN) with transferred learning

4.Dataset Description:

Chest X-ray dataset comprises 112,120 frontal-view X-ray images of 30,805 unique patients with the text-mined fourteen disease image labels (where each image can have multi-labels), mined from the associated radiological reports using natural language processing. Fifteen thoracic pathologies include - Atelectasis, Consolidation, Infiltration, Pneumothorax, Edema, Emphysema, Fibrosis, Effusion, Pneumonia, Pleural_thickening, Cardiomegaly, Nodule, Mass, Hernia and Coronavirus COVID-19.
Planning to have the training data into 16 different folders based on the classification of pathogens.

Contents:

1. 112,120 frontal-view chest X-ray PNG images in 1024*1024 resolution (under images folder)

2. Metadata for all images (Data_Entry_2017.csv): Image Index, Finding Labels, Follow-up #, Patient ID, Patient Age, Patient Gender, View Position, Original Image Size and Original Image Pixel Spacing.

3. Bounding boxes for ~1000 images (BBox_List_2017.csv): Image Index, Finding Label, Bbox[x, y, w, h]. [x y] are coordinates of each box's top left corner. [w h] represents the width and height of each box.

4. Two data split files (train_val_list.txt and test_list.txt) are provided. Images in the chest X-ray dataset are divided into these two sets on the patient level. All studies from the same patient will only appear in either training/validation or testing set.

COVID-19 Dataset:

- ✔ https://github.com/ieee8023/covid-chestxray-dataset/tree/master/images
- ✔ https://threadreaderapp.com/thread/1243928581983670272.html

5. *Exploratory Data Analysis (EDA)*

1) ***Downloading 45.7GB Data from NIHCC links –***

```
import urllib.request
from tqdm import tqdm
links = [
    'https://nihcc.box.com/shared/static/vfk49d74nhbxq3nqjg0900w5nvkorp5c.gz',
    'https://nihcc.box.com/shared/static/i28rlmbvmfjbl8p2n3ril0pptcmcu9d1.gz',
    'https://nihcc.box.com/shared/static/f1t00wrtdk94satdfb9olcolqx20z2jp.gz',
  'https://nihcc.box.com/shared/static/0aowwzs5lhjrceb3qp67ahp0rd1l1etg.gz',
    'https://nihcc.box.com/shared/static/v5e3goj22zr6h8tzualxfsqlqaygfbsn.gz',

  'https://nihcc.box.com/shared/static/asi7ikud9jwnkrnkj99jnpfkjdes7l6l.gz',
  'https://nihcc.box.com/shared/static/jn1b4mw4n6lnh74ovmcjb8y48h8xj07n.gz',
    'https://nihcc.box.com/shared/static/tvpxmn7qyrgl0w8wfh9kqfjskv6nmm1j.gz',
  'https://nihcc.box.com/shared/static/upyy3ml7qdumlgk2rfcvlb9k6gvqq2pj.gz',
  'https://nihcc.box.com/shared/static/l6nilvfa9cg3s28tqv1qc1olm3gnz54p.gz',
  'https://nihcc.box.com/shared/static/hhq8fkdgvcari67vfhs7ppg2w6ni4jze.gz',
  'https://nihcc.box.com/shared/static/ioqwiy20ihqwyr8pf4c24eazhh281pbu.gz'
]
for idx, link in tqdm(enumerate(links)):
    fn = 'images_%02d.tar.gz' % (idx+1)
    print ('downloading', fn, '...')
    urllib.request.urlretrieve(link, fn)  # download the zip file
print("Download complete. Please check the checksums")
```

```
# Count of images in each extracted "images_**" folders
from glob import glob

for i in ["%.2d" % i for i in range(1,13)]:
  folders = glob('/content/images_{}/images/*'.format(i))
  print('Number of images in images_{} folder is '.format(i),len(folders))
```

```
Number of images in images_01 folder is  4999
Number of images in images_02 folder is  10000
Number of images in images_03 folder is  10000
Number of images in images_04 folder is  10000
Number of images in images_05 folder is  10000
Number of images in images_06 folder is  10000
Number of images in images_07 folder is  10000
Number of images in images_08 folder is  10000
Number of images in images_09 folder is  10000
Number of images in images_10 folder is  10000
Number of images in images_11 folder is  10000
Number of images in images_12 folder is  7121
```

2) Building Project Folder structure and loading each class images to their respective folders

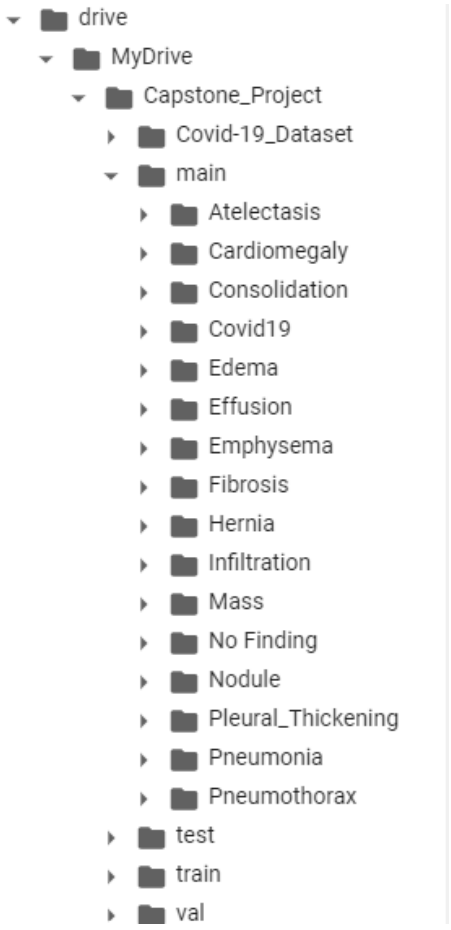

3) Dataset before Sampling

	Pathology	Images_Count
0	Atelectasis	11559
1	Cardiomegaly	2776
2	Effusion	13317
3	Infiltration	19894
4	Mass	5782
5	Nodule	6331
6	Pneumonia	1431
7	Pneumothorax	5302
8	Consolidation	4667
9	Edema	2303
10	Emphysema	2516
11	Fibrosis	1686
12	Pleural_Thickening	3385
13	Hernia	227
14	Covid19	1401
15	No Finding	60361

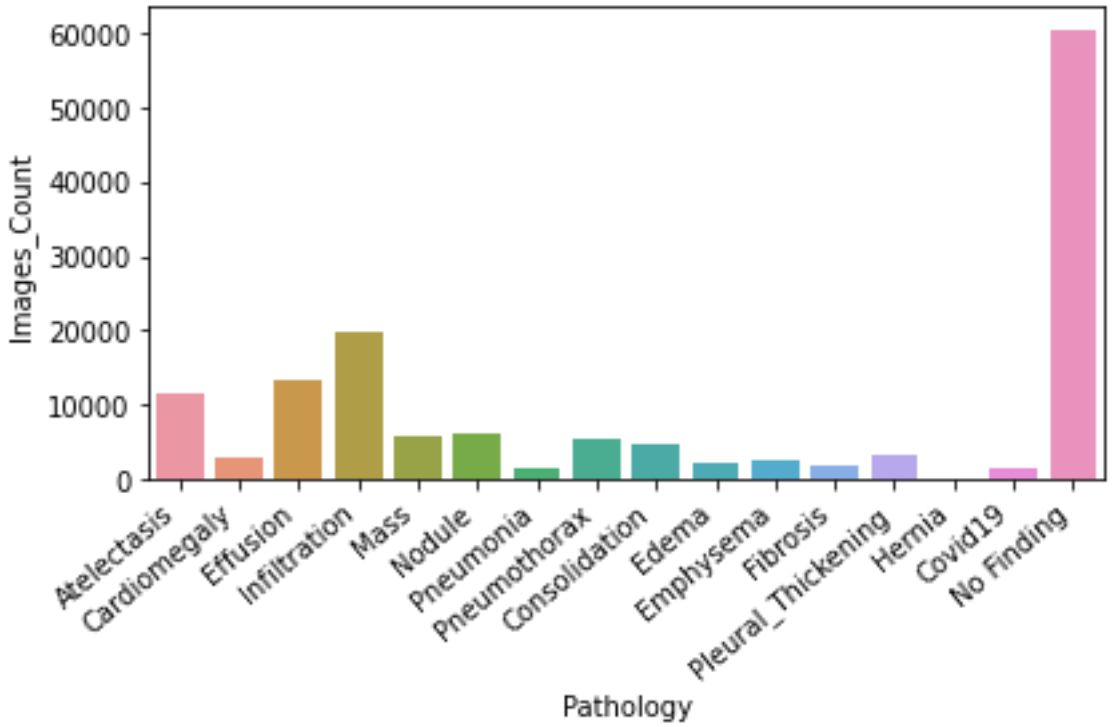

4) Dataset after Sampling (To make it balanced dataset)

	Pathology	Images_Count
0	Atelectasis	1400
1	Cardiomegaly	1400
2	Effusion	1400
3	Infiltration	1400
4	Mass	1400
5	Nodule	1400
6	Pneumonia	1400
7	Pneumothorax	1400
8	Consolidation	1400
9	Edema	1400
10	Emphysema	1400
11	Fibrosis	1400
12	Pleural_Thickening	1400
13	Hernia	227
14	Covid19	1401
15	No Finding	1400

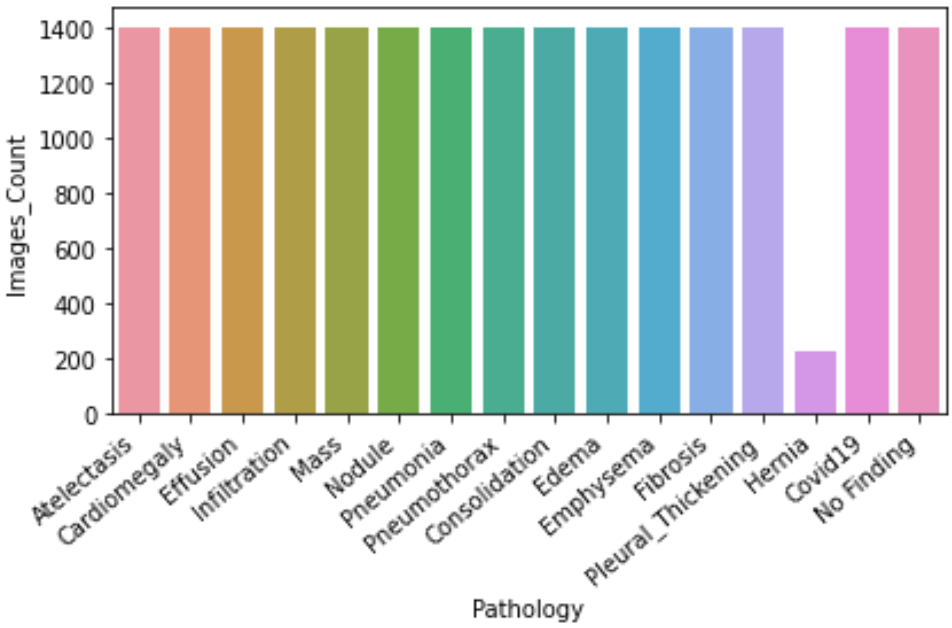

6 Early Results

We have explored three models so far and are still working on fine-tuning the models to get better accuracy and achieve better generalization.

Early Results from VGG16 Model –

```
#Training on the dataset
model_history = model.fit(x_train, y_train,
          batch_size=64,
          epochs=20,
          verbose=1,
          validation_data=(x_val, y_val))
```

```
Epoch 1/20
299/299 [==============================] - 3161s 11s/step - loss: 2.5498 - accuracy: 0.1869 - val_loss: 2.4907 - val_accuracy: 0.1851
Epoch 2/20
299/299 [==============================] - 3169s 11s/step - loss: 2.3323 - accuracy: 0.2365 - val_loss: 2.4283 - val_accuracy: 0.2058
Epoch 3/20
299/299 [==============================] - 3162s 11s/step - loss: 2.2434 - accuracy: 0.2700 - val_loss: 2.4600 - val_accuracy: 0.2148
Epoch 4/20
299/299 [==============================] - 3165s 11s/step - loss: 2.1708 - accuracy: 0.2859 - val_loss: 2.5273 - val_accuracy: 0.2129
```

Early Results from Chexnet Model –

```
#Training on the dataset
model_history = model.fit(x_train, y_train,
          batch_size=32,
          epochs=2,
          verbose=1,
          validation_data=(x_val, y_val))
```

```
Epoch 1/2
598/598 [==============================] - 961s 2s/step - loss: 3.5748 - accuracy: 0.0645 - val_loss: 3.4735 - val_accuracy: 0.0659
Epoch 2/2
598/598 [==============================] - 971s 2s/step - loss: 3.5717 - accuracy: 0.0630 - val_loss: 3.4735 - val_accuracy: 0.0659
```

Python Notebook Attachments –

1) Data Preparation


Covid_Data_setup.ipynb


Final_Data_Extraction_for_Pathology_Classifi

2) Finetuning using VGG16 Model


Capstone_Project_Final_Model_Building_VG

3) Finetuning using Chexnet Model


Capstone_Project_Final_Model_Building_Ch

References:

[1] Proto AV, Tocino I. Radiographic manifestations of lobar collapse. Semin Roentgenol. 1980;15 (2): 117-73. - Pubmed citation
[2] Amin H, Siddiqui WJ. Cardiomegaly. [Updated 2019 Jun 4]. In: StatPearls [Internet]. Treasure Island (FL): StatPearls Publishing; 2020 Jan-.
[3] Diaz-Guzman E, Dweik RA. Diagnosis and management of pleural effusions: a practical approach. Compr Ther. 2007 Winter. 33(4):237-46. [Medline].
[4] Li Deng and Dong Yu (2014), "Deep Learning: Methods and Applications", Foundations and Trends® in Signal Processing: Vol. 7: No. 3–4, pp 197-387.
[5] M. M. Najafabadi, F. Villanustre, T. M Khoshgoftaar, N. Seliya, R. Wald and E. Muharemagic, Deep learning applications and challenges in big data analytics, Journal of Big Data, 2 (1), 2015.
[6] CheXNet: Radiologist-Level Pneumonia Detection on Chest X-Ray with Deep Learning. arXiv:1711.05225v3 [cs.CV] 25 Dec 2017.
[7] Lorente Edgar. COVID-19 pneumonia - evolution over a week. https://radiopaedia.org/cases/COVID-19-pneumonia-evolution-over-a-week-1?lang=us.
[8] Bai H.X., Hsieh B. Performance of radiologists in differentiating COVID-19 from viral pneumonia on chest CT. Radiology. 2020 200823. [Google Scholar].
[9] Pahal P, Avula A, Sharma S. Emphysema. [Updated 2019 Dec 31]. In: StatPearls [Internet]. Treasure Island
[10] Iqbal MA, Gupta M. Cardiogenic Pulmonary Edema. [Updated 2020 Mar 18]. In: StatPearls [Internet]. Treasure Island
[11] Krishna R, Ullah S. Idiopathic Pulmonary Fibrosis. [Updated 2019 Jan 11]. In: StatPearls [Internet]. Treasure Island
[12] Cherian, Thomas, Mulholland, E Kim, Carlin, John B, Ostensen, Harald, Amin, Ruhul, Campo, Margaret de, Greenberg, David, Lagos, Rosanna, Lucero, Marilla, Madhi, Shabir A, et al. Standardized interpretation of paediatric chest radiographs for the diagnosis of pneumonia in epidemiological studies. Bulletin of the World Health Organization, 83(5):353{359, 2005.
[13] Franquet, T. Imaging of pneumonia: trends and algorithms. European Respiratory Journal, 18(1):196{208, 2001.
[14] Huang, Gao, Liu, Zhuang, Weinberger, Kilian Q, and van der Maaten, Laurens. Densely connected convolutional networks. arXiv preprint arXiv:1608.06993, 2016.
[15] Deng, Jia, Dong, Wei, Socher, Richard, Li, Li-Jia, Li, Kai, and Fei-Fei, Li. Imagenet: A large-scale hierarchical image database. In Computer Vision and Pattern Recognition, 2009. CVPR 2009. IEEE Conference on, pp. 248{255. IEEE, 2009.
[16] Kingma, Diederik and Ba, Jimmy. Adam: A method for stochastic optimization. arXiv preprint arXiv:1412.6980, 2014.
[17] Rajpurkar, Pranav, Hannun, Awni Y, Haghpanahi, Masoumeh, Bourn, Codie, and Ng, Andrew Y. Cardiologist-level arrhythmia detection with convolutional neural networks. arXiv preprint arXiv:1707.01836, 2017.
[18] Raoof, Suhail, Feigin, David, Sung, Arthur, Raoof, Sabiha, Irugulpati, Lavanya, and Rosenow, Edward C. Interpretation of plain chest roentgenogram. CHEST Journal, 141(2):545{558, 2012.
[19] Neuman, Mark I, Lee, Edward Y, Bixby, Sarah, Diperna, Stephanie, Hellinger, Je_rey, Markowitz, Richard, Servaes, Sabah, Monuteaux, Michael C, and Shah, Samir S. Variability in the interpretation of chest radiographs for the diagnosis of pneumonia in children. Journal of hospital medicine, 7(4): 294{298, 2012.
[20] Islam, Mohammad Tariqul, Aowal, Md Abdul, Minhaz, Ahmed Tahseen, and Ashraf, Khalid. Abnormality detection and localization in chest x-rays using deep convolutional neural networks. arXiv preprint arXiv:1705.09850, 2017.

[21] Ioffe, Sergey and Szegedy, Christian. Batch normalization: Accelerating deep network training by reducing internal covariate shift. In International Conference on Machine Learning, pp. 448{456, 2015.
[22] Grewal, Monika, Srivastava, Muktabh Mayank, Kumar, Pulkit, and Varadarajan, Srikrishna. Radnet: Radiologist level accuracy using deep learning for hemorrhage detection in ct scans. arXiv preprint arXiv:1710.04934, 2017.
[23] Zhou, Bolei, Khosla, Aditya, Lapedriza, Agata, Oliva, Aude, and Torralba, Antonio. Learning deep features for discriminative localization. In Proceedings of the IEEE Conference on Computer Vision and Pattern Recognition, pp. 2921{2929, 2016.
[24] Yao, Li, Poblenz, Eric, Dagunts, Dmitry, Covington, Ben, Bernard, Devon, and Lyman, Kevin. Learning to diagnose from scratch by exploiting dependencies among labels. arXiv preprint arXiv:1710.10501, 2017.
[25] Wang, Xiaosong, Peng, Yifan, Lu, Le, Lu, Zhiyong, Bagheri, Mohammadhadi, and Summers, Ronald M. Chest x-ray8: Hospital-scale chest x-ray database and benchmarks on weakly-supervised classi_cation and localization of common thorax diseases. arXiv preprint arXiv:1705.02315, 2017.
[26] Davies, H Dele, Wang, Elaine E-l, Manson, David, Babyn, Paul, and Shuckett, Bruce. Reliability of the chest radiograph in the diagnosis of lower respiratory infections in young children. The Pediatric infectious disease journal, 15(7):600{604, 1996.
[27] Esteva, Andre, Kuprel, Brett, Novoa, Roberto A, Ko, Justin, Swetter, Susan M, Blau, Helen M, and Thrun, Sebastian. Dermatologist-level classi_cation of skin cancer with deep neural networks. Nature, 542(7639):115{118, 2017.
[28] Hopstaken, RM, Witbraad, T, Van Engelshoven, JMA, and Dinant, GJ. Inter-observer variation in the interpretation of chest radiographs for pneumonia in community-acquired lower respiratory tract infections. Clinical radiology, 59(8):743{752, 2004.
[29] Potchen, EJ, Gard, JW, Lazar, P, Lahaie, P, and Andary, M. E_ect of clinical history data on chest film interpretation-direction or distraction. In Investigative Radiology, volume 14, pp. 404{404, 1979.
[30] Lakhani, Paras and Sundaram, Baskaran. Deep learning at chest radiography: Automated classification of pulmonary tuberculosis by using convolutional neural networks. Radiology, pp. 162326, 2017.
[31] Y. Bar, I. Diamant, L. Wolf, S. Lieberman, E. Konen, and H. Greenspan, “Chest pathology identification using deep feature selection with non-medical training,” Comput. Methods Biomech. Biomed. Eng. Imaging Vis., vol. 6, no. 3, pp. 259–263, 2018, doi: 10.1080/21681163.2016.1138324.
[32] M. T. Islam, M. A. Aowal, A. T. Minhaz, and K. Ashraf, “Abnormality Detection and Localization in Chest X-Rays using Deep Convolutional Neural Networks,” 2017, [Online]. Available: http://arxiv.org/abs/1705.09850
[33] S. Basu, S. Mitra, and N. Saha, “Deep Learning for Screening COVID-19 using Chest X-Ray Images,” pp. 1–6, 2020, [Online]. Available: http://arxiv.org/abs/2004.10507.
[34] NHS England, “Diagnostic Imaging Dataset Statistical Release,” NHS Engl., pp. 1–18, 2017, [Online].Available:https://www.england.nhs.uk/statistics/wpcontent/uploads/sites/2/2015/08/Provisional-Monthly-Diagnostic-Imaging-DatasetStatistics-2016-03-17.pdf.